

Automated CT Segmentation of Diseased Hip Using Hierarchical and Conditional Statistical Shape Models

Futoshi Yokota¹, Toshiyuki Okada², Masaki Takao², Nobuhiko Sugano²,
Yukio Tada³, Noriyuki Tomiyama², and Yoshinobu Sato²

¹ Graduate School of Engineering, Kobe University, Japan

² Graduate School of Medicine, Osaka University, Japan
yoshi@image.med.osaka-u.ac.jp

³ Graduate School of System Informatics, Kobe University, Japan

Abstract. Segmentation of the femur and pelvis is a prerequisite for patient-specific planning and simulation for hip surgery. Accurate boundary determination of the femoral head and acetabulum is the primary challenge in diseased hip joints because of deformed shapes and extreme narrowness of the joint space. To overcome this difficulty, we investigated a multi-stage method in which the hierarchical hip statistical shape model (SSM) is initially utilized to complete segmentation of the pelvis and distal femur, and then the conditional femoral head SSM is used under the condition that the regions segmented during the previous stage are known. CT data from 100 diseased patients categorized on the basis of their disease type and severity, which included 200 hemi-hips, were used to validate the method, which delivered significantly increased segmentation accuracy for the femoral head.

1 Introduction

Segmentation of the femur and pelvis is a prerequisite for patient-specific planning and simulation for hip surgery. Although healthy hips might be relatively easy to segment, it is more important to work with diseased hips for clinical applications. Bone deformation and joint-space narrowing are very severe in diseased hips, and additional lesions such as cysts often develop; therefore, the boundaries of the femur and pelvis around the joint space are often difficult to identify from images. We aim to achieve automated segmentation using CT images of hips deformed due to disease.

Statistical shape models (SSMs) typically have been used to perform automated segmentation of hip joints. A previous study regarding pelvis segmentation determined from CT reported that the segmentation accuracy was insufficient around the joint space because of the lack of boundary information [1]. Some previous studies that addressed both the pelvis and femur have proposed methods based on the ball-and-socket joint kinematics of the hip [2,3]. In these methods, the femoral head is assumed to be approximated by a spherical shape;

however, sphere approximation is often inappropriate for the diseased hip joint. Although these studies also used the Newtonian-dynamics based method [3] and graph-cut based method [4] to address the regional overlap issue of the pelvic and femoral bones, these methods did not incorporate anatomical priors in localizing ambiguous boundaries. One interesting point is that these two independent papers reported that segmentation accuracy was lower for the femoral head than for the acetabulum [2,3]. We proposed a hierarchical SSM of the hip to perform segmentation of the diseased hips [5]. In our method, a combined SSM consisting of the acetabulum patch and femoral head patch was successfully used to impose anatomical consistency. However, occasionally, achieving weight balance was difficult in the simultaneous optimization of the combined SSM and independent pelvis and femur SSMs. In addition, computational cost was a problem as well. In few studies, statistical prediction methods using partial least squares (PLS) and conditional SSMs were used as different approaches to predict bone shape from adjacent bone shapes for the shoulder [6] and the vertebra [7]; although these methods were useful for working with joint structures, they did not prove useful in segmentation.

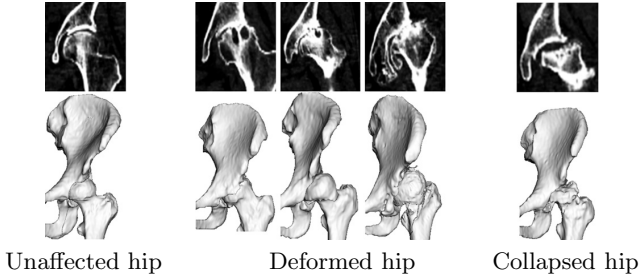
On the basis of the above literature survey, previous efforts remain insufficient for Segmentation of the diseased hips. Hierarchical anatomical constraints would be useful, but occasionally, simultaneous optimization causes instability [5]. Because two independent groups have reported that segmentation accuracy was better for the acetabulum than for the femur [2,3], statistical prediction [6,7] of the femur from the (pre-segmented) acetabulum might be useful. On the basis of these observations, we propose a method that combines a hierarchical SSM with a conditional SSM. The following are the major contributions of this paper: (1) A simpler version of the hierarchical hip SSM [5] and then a conditional (proximal) femur SSM [7] under the condition that the pelvis and distal femur are already segmented, are used to improve segmentation accuracy of the femur. (2) CT data of 100 diseased patients categorized on the basis of their disease type and severity, which included 200 hemi-hips, are used to validate the proposed method. To our knowledge, the work of Zoroofi [8] is the only study that validated diseased hip segmentation in 60 cases with disease categorization used conventional image analysis techniques; however validation was not successful in a few portions of the diseased hips.

2 Dataset

In this study, 200 hemi-hips of 100 female patients who underwent total hip arthroplasty (THA) surgery were included in the data set. In these patients, one side was not diseased (hereafter, the hips have been termed the “unaffected hip”) and the other side was diseased (hereafter, the hips have been termed the “diseased hip”). Table 1 presents the disease categories of the 100 diseased hips. We categorized the diseased hips as either a deformed hip (osteoarthritis of the hip) or as a collapsed hip (mostly avascular necrosis of the femoral head). The deformed hips were primarily affected by secondary osteoarthritis, and their

Table 1. Number of cases in each disease category

Category of disease			Number of cases
Deformed hip	Primary osteoarthritis		7
	Secondary osteoarthritis	Crowe 1	58
		Crowe 2, 3, 4	24
Collapsed hip	Avascular necrosis of the femoral head	10	
	Rapidly destructive coxarthropathy	1	

**Fig. 1.** Coronal views and 3D renderings of CT images of the unaffected and diseased hips. Upper: Coronal views. Lower: 3D renderings.

shape deformation revealed a characteristic tendency as the disease progressed. In 24 of these cases, the Crowe classifications of disease were 2, 3 or 4 (larger values denote more serious conditions), and the femoral head was highly deformed. Fig. 1 presents coronal views and 3D rendering of the CT data for the unaffected and diseased hips. In the unaffected hip, separation of the femoral head and acetabulum by the joint space were observed. However, in the diseased hip, the femoral head was highly deformed, and identification of the joint space on the basis of the local image features alone was difficult.

3 Methods

The proposed segmentation method consists of two stages, in which the hierarchical hip SSM is initially used to complete segmentation of the pelvis and distal femur, and subsequently, the conditional femoral head SSM (FH-SSM) is used under the condition that the regions segmented during the previous stage are known.

3.1 Femur and Pelvis Segmentation Using the Hierarchical Hip SSM

A simpler version of the hierarchical SSM was used to perform coarse-to-fine segmentation [5]; we simplify the original formulation described in that study by removing the consistency constraint among the independent femur and pelvis

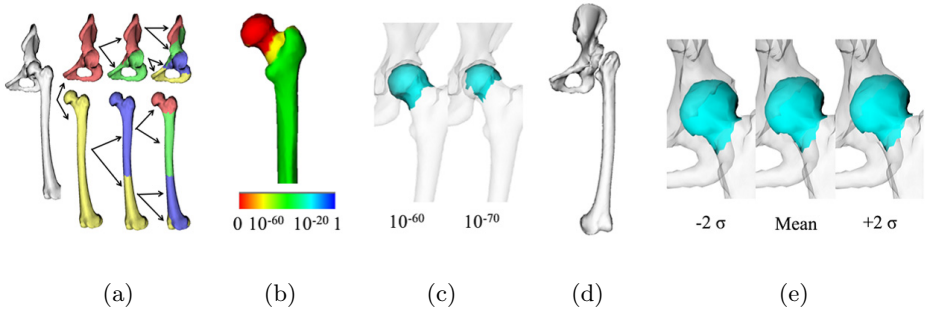


Fig. 2. Hierarchical hip SSM and conditional FH-SSM. (a) Hierarchical hip SSM. (b) p-value map on the basis of CCA of the femur surface influenced by the pelvis. Small values denote high correlation with the pelvis. (c) Femoral head region (presented in cyan) obtained by thresholding the p-value map. (d) Condition surface comprising of the pelvis and distal femur. Note that the femoral head is not included. (e) First mode of constructed conditional FH-SSM.

SSMs and cascading the pelvis and femur segmentations. The hierarchical SSM comprises the combined pelvis and femur SSM at the first level of hierarchy, the independent pelvis and femur SSMs are at the second level, and each bone is divided into multiple patches at the third level (Fig. 2 (a)). In preparing the training shapes, pair-wise surface registration using non-rigid registration [9] is performed to determine the shape correspondences between the individual and average pelvis and femur. As a preparation, our proposed method is used to automatically localize the pelvic coordinate system [10]. After this localization, hierarchical segmentation is performed. Initially, SSM initialization is performed. The combined femur and pelvis SSM (top level in Fig. 2 (a)) is fitted to the boundary edge points of the roughly segmented bone regions extracted by using simple thresholding of CT images to obtain initial parameter settings for subsequent segmentation processes. The joint flexibility is modeled as shape variations in the combined femur and pelvis SSM; the fitting results of this are inherited to subsequent independent pelvis and femur SSMs fitting (second level in Fig. 2 (a)) by providing their initial parameters. Next, segmentation of the pelvis is performed by pelvis SSM fitting and subsequent divided-patch SSM fitting (third and fourth levels of the upper row in Fig. 2 (a)) to perform coarse-fine refinement. Because it has been reported that accuracy was better for the pelvis than for the femur in previous studies [2,3], we first segment the pelvis and then segment the femur. Each SSM fitting is performed using an iterative method. Edge detection is performed on the basis of the intensity profile analysis along the perpendicular direction at each surface point of SSM that is estimated at the previous iteration, and SSM fitting to the detected edges is repeated for a fixed number of times. Finally, segmentation of the femur is similarly performed by femur SSM fitting. To avoid the overlap of the pelvis and femoral head regions, we search the femoral head edges only outside the presegmented pelvic regions.

3.2 Refinement of Femoral Head Segmentation Using Conditional SSM

To improve the segmentation accuracy of the femur, a conditional SSM is used to perform segmentation assuming that the pelvis and distal femur have already been segmented, and their segmentation accuracy is better than the femoral head, particularly at the previous segmentation stage. Bruijne's method [7] combined with patch extent determination using canonical correlation analysis (CCA) is used to construct the conditional FH-SSM.

In our application of a conditional SSM, it is necessary to determine the extent of the femoral head to be conditionally modeled. To do so, a CCA-based method is used. CCA is used to determine the patch extent of the femoral head by selecting the area revealing a high correlation with the pelvis. In the previous method [11], CCA was used to define a p-value map on a single-organ surface, which revealed the significance level of the correlation between each point of the surface and one specified point. We extend the method so that multiple structures can be examined. Let S_f denote the shape of the femur and S_p denote the pelvis. We calculate the p-value of CCA for all the pairs of points between S_f and S_p . As a result, for each point x_i on S_p , the p-value on S_f is obtained, which we denote as $p(S_f; x_i \in S_p)$. We define the p-value map on S_f for S_p as

$$p(S_f; S_p) = \arg \min_{x_i \in S_p} p(S_f; x_i) \quad (1)$$

Fig. 2 (b) presents the p-value map of Eq. (1) obtained from the training data. The areas where the p-values are small represent the strong correlations with the pelvis. If the p-value at a point on S_f is less than a predetermined significance level, the point is regarded as having a significant correlation with S_p . Fig. 2 (c) presents several results of the thresholded p-value map. We select the optimal threshold by cross-validation within the training dataset. The thresholded region is used for the femoral head region, whereas the pelvis and distal femur region are used for the condition part of the conditional SSM, which is described below.

According to [7], let X denote the shape of the femoral head, and Y denote the combined shape of the pelvis and distal femur. The distribution is given by $P(X|Y = Y_0)$, which is the conditional distribution of a shape of X given a shape $Y = Y_0$ that is segmented during the previous stage

$$P(X|Y = Y_0) = N(\mu_{X|Y_0}, \Sigma_{X|Y_0}) \quad (2)$$

with

$$\mu_{X|Y_0} = \mu_X + \Sigma_{XY} \Sigma_{YY}^{-1} (Y_0 - \mu_Y), \quad (3)$$

$$\Sigma_{X|Y_0} = \Sigma_{XX} - \Sigma_{XY} \Sigma_{YY}^{-1} \Sigma_{YX}. \quad (4)$$

Where μ_X and μ_Y are the mean shapes of the training datasets of X and Y , and the covariances Σ_{ij} are obtained from the combined covariance matrix

$$\Sigma = \begin{bmatrix} \Sigma_{XX} & \Sigma_{XY} \\ \Sigma_{YX} & \Sigma_{YY} \end{bmatrix} = \begin{bmatrix} Cov(X, X) & Cov(X, Y) \\ Cov(Y, X) & Cov(Y, Y) \end{bmatrix}. \quad (5)$$

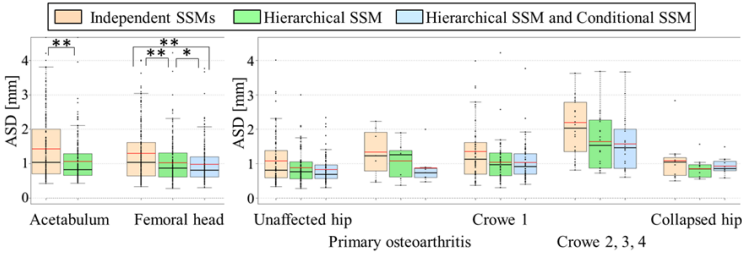


Fig. 3. Evaluation results for segmentation accuracy. Left: Box-plots of the average symmetric surface distance (ASD) around the acetabulum and femoral head for each SSM. Right: Box-plots of ASD around the femoral head in each disease category. The black and red horizontal lines in the box display the median and mean values, respectively. * and ** = significant improvement; * = $0.01 < p < 0.05$; ** = $p < 0.01$.

Fig. 2 (e) presents the constructed conditional FH-SSM under the condition shape depicted in Fig. 2 (d). The method described in 3.1 is similarly used to perform segmentation of the femoral head by conditional FH-SSM fitting.

4 Results

We used the 100 CT data from the 100 female patients (200 hemi-hips) described in Section 2. 2-fold cross validations were performed to evaluate the segmentation accuracy. In the 2-fold cross validation, the dataset was randomly divided into two groups, and then one group was used for training and parameter tuning and the other for testing. In the training phase, leave-one-out cross validation was performed to optimize the parameters involved in SSM construction and segmentation within the training data. The training and testing datasets were swapped and validation was performed in the same way. The optimal p-value threshold from the CCA analysis for patch extent determination was $p = 10^{-60}$ and $p = 10^{-70}$ in the two training datasets.

Figure 3 presents the accuracy evaluation results of one conventional method, the independent pelvis and femur SSMs (the femur SSM was performed after the pelvis SSM); two stages of the proposed method, the hierarchical hip SSM, and combined hierarchical hip SSM with conditional FH-SSM. Manually traced boundaries were used for the gold standard, and the average symmetric surface distance (ASD) between the estimated and gold standard surfaces was used for an error measure. To evaluate the efficacy of the proposed method, we measured the accuracy around the joint space. When we used the conventional method, additional manual specification in the CT images was necessary to determine the femur coordinate system. Around the acetabulum, ASD was 1.43 mm in the previous method and 1.06 mm in the hierarchical hip SSM. Around the femoral head, ASD was significantly reduced in the combined hierarchical hip SSM with conditional FH-SSM (0.97 mm) compared with that in the previous method (1.30 mm, $p < 0.01$) and the hierarchical hip SSM (1.02 mm, $p < 0.05$). In each

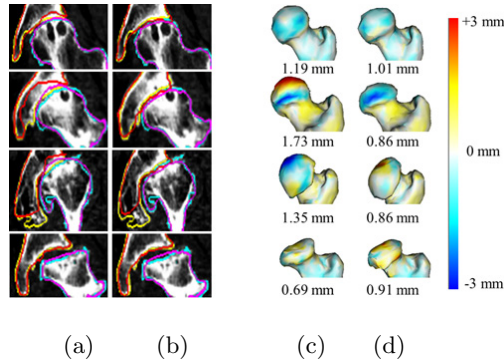


Fig. 4. Results of illustrative cases. (a) and (b) show coronal views. (c) and (d) show 3D renderings and ASDs. (a) and (c) show results from the conventional independent pelvis and femur SSMs. (b) and (d) are results from the hierarchical hip SSM and conditional FH-SSM. The red and magenta contours correspond to the estimated regions of the pelvis and femur, respectively. The yellow and cyan contours are gold standards.

disease category, ASDs were 0.83 mm in the unaffected hip, 1.12 mm in the diseased hip, 1.15 mm in the deformed hip, and 0.92 mm in the collapsed hip.

Figure 4 presents coronal views and 3D renderings of few typical cases. We confirmed that the hierarchical hip SSM effectively worked to maintain the consistency between the acetabulum and femoral head boundaries. In addition, the accuracy of the femoral head was slightly improved in the conditional FH-SSM relative to that in the hierarchical hip SSM. The total computational times were about 10 min in the independent SSMs, 13 min in the combined hierarchical SSM, and 15 min in the combined SSM with conditional SSM (3.0-GHz CPU with 16-GB RAM).

5 Discussion and Conclusions

In this study, we investigated a method that cascades the use of a hierarchical hip SSM and conditional FH-SSM combined with CCA-based patch extent determination. In addition, we used CT data from 100 diseased patients categorized on the basis of disease type and severity, which included 200 hemi-hips, to validate the method. Significant improvement was confirmed by use of the conditional FH-SSM after the hierarchical hip SSM. Although it has been reported that the accuracy of the femoral head was lower than that of the acetabulum in [2,3], we observed that the accuracies for the femoral head and acetabulum were comparable in our results. Although ASD of the diseased hips was 1.12 mm, which was worse than the 0.83 mm value of the unaffected hips, it is an acceptable level, considering that our dataset comprised several highly deformed hips. In the third row of Fig. 4, the accuracy of the bony spur was depicted to be insufficient. In the fourth row, the accuracy was reduced in the collapsed hip in the

conditional FH-SSM. We consider that these types of disease deformation might not be captured by a single SSM. In future work, we plan to construct SSMs for each disease category and to propose a method for automatically detecting a suitable SSM appropriate for a particular disease type.

Acknowledgement. This work is partly supported by MEXT Grand-in-Aid for Scientific Research No. 21103003 and No. 25242051.

References

1. Seim, H., Kainmueller, D., Heller, M., Lamecker, H., Zachow, S., Hege, H.C.: Automatic Segmentation of the Pelvic Bones from CT Data Based on a Statistical Shape Model. In: Eurographics Workshop on Visual Computing for Biomedicine, pp. 93–100 (2008)
2. Kainmueller, D., Lamecker, H., Zachow, S., Hege, H.C.: An Articulated Statistical Shape Model for Accurate Hip Joint Segmentation. In: Conf. Proc. IEEE Eng. Med. Biol. Soc., pp. 6345–6351 (2009)
3. Schmid, J., Kim, J., Magnenat-Thalmann, N.: Robust statistical shape models for MRI bone segmentation in presence of small field of view. *Med. Image Anal.* 15(1), 155–168 (2011)
4. Kainmueller, D., Lamecker, H., Zachow, S., Hege, H.-C.: Coupling Deformable Models for Multi-object Segmentation. In: Bello, F., Edwards, E. (eds.) ISBMS 2008. LNCS, vol. 5104, pp. 69–78. Springer, Heidelberg (2008)
5. Yokota, F., Okada, T., Takao, M., Sugano, N., Tada, Y., Sato, Y.: Automated segmentation of the femur and pelvis from 3D CT data of diseased hip using hierarchical statistical shape model of joint structure. In: Yang, G.-Z., Hawkes, D., Rueckert, D., Noble, A., Taylor, C. (eds.) MICCAI 2009, Part II. LNCS, vol. 5762, pp. 811–818. Springer, Heidelberg (2009)
6. Yang, Y.M., Rueckert, D., Bull, A.: Predicting the shapes of bones at a joint: application to the shoulder. *Comput. Methods Biomech. Biomed. Engin.* 11(1), 19–30 (2008)
7. de Bruijne, M., Lund, M.T., Tanko, L.B., Pettersen, P.C., Nielsen, M.: Quantitative vertebral morphometry using neighbor-conditional shape models. *Med. Image Anal.* 11(5), 503–512 (2007)
8. Zoroofi, R.A., Sato, Y., Sasama, T., Nishii, T., Sugano, N., Yonenobu, K., Yoshikawa, H., Ochi, T., Tamura, S.: Automated Segmentation of Acetabulum and Femoral Head From 3-D CT Images. *IEEE Trans. Inf. Technol. Biomed.* 7(4), 329–343 (2003)
9. Rueckert, D., Sonoda, L.I., Hayes, C., Hill, D.L.G., Leach, M.O., Hawkes, D.J.: Non-rigid registration using freeform deformations: Application to breast MR images. *IEEE Trans. Med. Image* 18(8), 712–721 (1999)
10. Yokota, F., Okada, T., Takao, M., Sugano, N., Tada, Y., Tomiyama, N., Sato, Y.: Automated Localization of Pelvic Anatomical Coordinate System from 3D CT Data of the Hip Using Statistical Atlas. *Med. Imag. Tech.* 30(1), 43–52 (2012) (in Japanese)
11. Fillard, P., Pennec, X., Thompson, P.M., Ayache, N.: Evaluating Brain Anatomical Correlations via Canonical Correlation Analysis of Sulcal Lines. In: MICCAI 2007 Workshop: Statistical Registration, HAL-CCSD (2008)